INTERNATIONAL JOURNAL OF OPTIMIZATION IN CIVIL ENGINEERING
Int. J. Optim. Civil Eng., 2020; 10(3):365-389

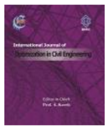

SWITCHING TEAMS ALGORITHM FOR SIZING OPTIMIZATION OF TRUSS STRUCTURES

M. Shahrouzi*, †
Civil Engineering Department, Faculty of Engineering, Kharazmi University, Tehran, Iran

ABSTRACT

Meta-heuristics have received increasing attention in recent years. The present article introduces a novel method in such a class that distinguishes a number of artificial search agents called players within two teams. At each iteration, the active player concerns some other players in both teams to construct its special movements and to get more score. At the end of some iterations (like quarters of a sports game) the teams switch their places for fair play. The algorithm is developed to solve a general purpose optimization problem; however, in this article its application is illustrated on structural sizing design. *Switching Teams Algorithm* is presented as a parameter-less population-based algorithm utilizing just two control parameters. The proposed method can recover diversity in a novel manner compared to other meta-heuristics in order to capture global optima.

Keywords: new meta-heuristic algorithm; constrained optimization; parameter-less method; structural design.

Received: 10 January 2020; Accepted: 15 May 2020

1. INTRODUCTION

Many engineering fields deal with complexity in their optimization problems. Structural design is one of the most famous fields among them that have received considerable research attention from early 19's century up to now. It is usually characterized by non-differentiable functions and narrow non-convex feasible regions with respect to the entire design space.

Two main categories of solution means are most popular for optimization. Mathematical Programming constitutes the first category; best suited for analytical differentiable functions

---

*Corresponding author: Civil Engineering Department, Faculty of Engineering, Kharazmi University, Tehran, Iran
†E-mail address: shahruzi@khu.ac.ir (M. Shahrouzi)

and convex programming problems. However, the second including meta-heuristics, mostly works with sampling of the function itself without the need to evaluate any its gradients. Such a feature have made it interesting for several practical fields; including civil engineering problems. Another reason for popularity of meta-heuristics application in structural engineering, is complexity of the corresponding continuous and discrete problems that brings about the need for efficient methods to reveal even a near-optimal solution in practical time. That is why several research works have already been addressed in this field. Some of the applied methods can be referred as Evolutionary Algorithms [1–3], Simulated Annealing[4,5], Ant Colony and swarm intelligence [6–8], Harmony Search [9–12], Charged System Search [13–15], Colliding Bodies Optimization [16], Imperialist Competition [17–19], Teaching–Learning-Based Optimization [20,21], Water Evaporation Optimization [22], Thermal Exchange Optimization [23], Grey Wolf Optimizer [24], Interior Search Algorithm [25], Cuckoo Search [26], Sine-Cosine Algorithm [27,28] and Vibrating Particles Search [29].

An important issue for meta-heuristic algorithms is the way each applies to provide intensification and diversification [30]. In some vast design spaces, it is desired to have powerful intensification toward the solution to provide computational efficiency in finding a practical solution. However, in some others overpassing local optima toward global optimum may have considerable merit in cost minimization. It is ideal to have an algorithm that can robustly balance these features when working with different design spaces. The matter is sometimes implemented via problem-specific parameter tuning. However, a practical strategy is to employ more robust operators in the algorithm, instead of dealing with extra computational effort in challenging task of parameter tuning.

The present work introduces a novel meta-heuristic algorithm regarding the aforementioned goals. It simulates some actions of sports game players in the opposite teams that alternatively switch their position to provide sufficient diversity. The method is called *Switching Teams Algorithm.* STA is proposed here as a parameter-less population-based algorithm working with no more than population size and number of function evaluations. It is validated here-in-after by solving a number of structural sizing benchmarks that include both continuous and discrete design spaces in a variety of small to large-scale examples.

2. SWITCHING TEAMS ALGORITHM: CONCEPTS AND STEPS

A new meta-heuristic algorithm is introduced that is inspired by some actions in sports' games between two teams in the opposite sides. In view of a player, the others are either in its team or in the opposite. It will of-course affect the forthcoming play-strategy. When deciding to move, a player may concentrate on one of the local neighbor's; however, the overall movement of either team is also observed as each team wears its special color. A more experienced player; namely the *captain* also takes place in the middle of the team so that he can better communicate with its-team players. During the game, each player can run back if the new position is worse than the previous. A player has also an insight on the way that its captain instructs. The teams should switch their ground at the end of each round of the game. It will help diversifying priority of the environmental conditions between both; rather than limiting them to one. For example, the direction of sun shine affects the players' visibility. It will then exerts some type of priority on the ground position for a team when selecting the side. As the game time is consumed, the sun gradually changes position over the horizon affecting such priority.

The present optimization algorithm is designated to take merit of such movement strategies in the artificial search space. Each player simulates an agent (a design vector) that seeks for the best opportunity (merit) by running from one position to another. The entire population of search agents is thus divided into two teams with equal number of players. Effect of the environment in selecting the side, is modeled via sorting the population based on a merit function evaluated over the corresponding design vectors.

The above concepts and more are simulated hereinafter to develop a novel optimization method called *Switching-Teams Algorithm*, STA via the following steps.

1. STA is a population-based method, so the first step is initiating the players as:

$$X_i = X^{LB} + rand \otimes (X^{UB} - X^{LB}) \tag{1}$$

The vector X_i is the i^{th} player randomly positioned in the range $[X^{LB}, X^{UB}]$ indicating lower and upper bounds on design vector, respectively. The function *rand* generates a random vector with positive components less than unity and $\otimes$ stands for the element-wise multiplication.

2. Evaluate the fitness (merit) function for all N_p players in the population of two teams.
3. Sort the players due to their fitness values. Determine the ball position; X_B as the best experience of the entire population.
4. *Switching the sides*: Sort the entire population due to fitness scores. Consider two teams; one of them named as the *friend team* and the other as the *enemy*. By a prescribed *switching probability* assign either the fitter side (half population) to the friend team and the other to the enemy or vice versa. Median player of each team is called its *captain*.
5. For each player in the friend team, do
   a. *Locally directed run*: The player pays attention on a randomly chosen player in its team (its neighbor) and determine a decision factor d based on priority of such a neighbor position over the current. If the neighbor is fitter than the player, set d to 1; otherwise set it to -1. The run vector is then generated as:

$$V_i^{\mathrm{I}} = d.(X_j - X_i) \tag{2}$$

   b. *Globally directed run*: The player takes an insight on the overal movement of the teams. If $d = 1$, set a run vector V_i^{II} as the direction in which mean of the 1st team moves toward the best position X_B; otherwise set V_i^{II} in direction from mean of the 2nd team toward X_B.
   c. *Move* the player to the following new candidate position and evaluate its fitness.

$$X_i \leftarrow X_i + rand \otimes V_i^{\mathrm{I}} + rand \otimes V_i^{\mathrm{II}} \tag{3}$$

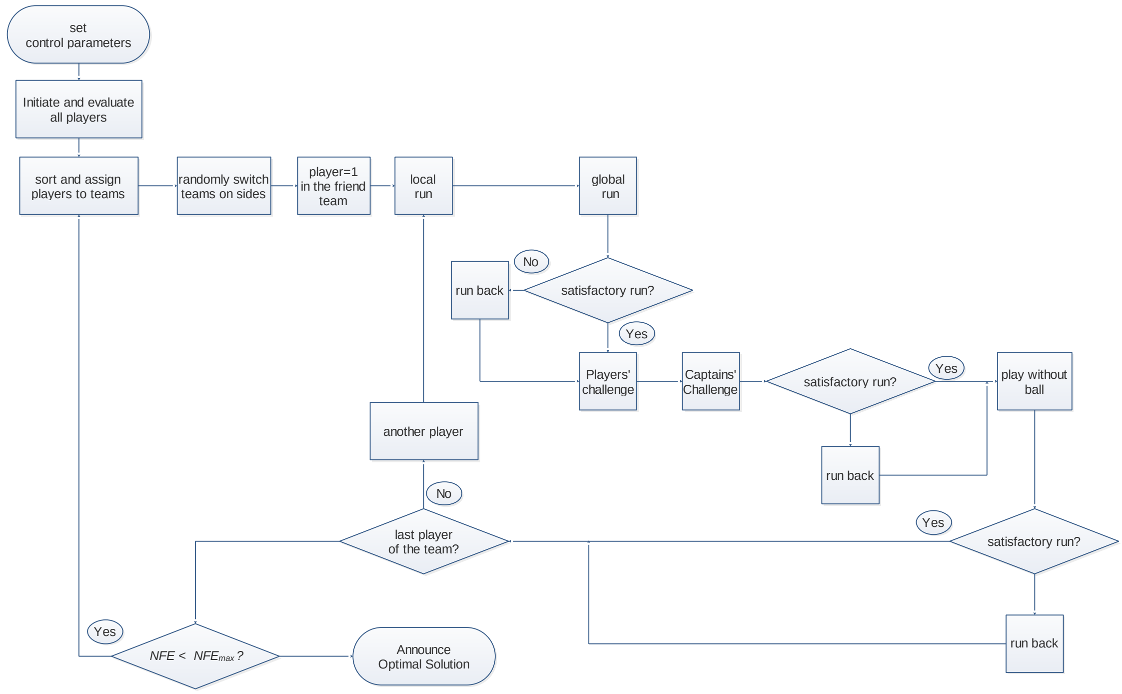

Figure 1. Flowchart of the proposed STA

d. *Running back*: Move the current player back to its previous postion if it is fitter than the new position
e. *Players' challenge*: when both a random player in the enemy team, denoted by X'_k, and the current player think to posess the ball; construct the following move direction:

$$V_i^{\text{III}} = X_B - X_k^{'} - X_i \tag{4}$$

f. *Captains' challenge*: Denote captain of the friend team as X_c and the other as X'_c and construct their challenge direction as:

$$V_i^{\text{IV}} = X_C - X_C^{'} \tag{5}$$

g. Make another run by the current player by:

$$X_i \leftarrow X_i + rand \otimes V_i^{\text{III}} + rand \otimes V_i^{\text{IV}} \tag{6}$$

h. *Running back*: Move the current player back to its previous postion if it is fitter than the new position.
i. *Diverse playing without the ball*: By equal chance the current player selects one of the two targets to run toward: either mirror of its position in the ground or position of a randomly chosen player in the enemy team, X'_k:

$$X_i \leftarrow rand \otimes \begin{cases} X_k^{'} \\ X^{LB} + X^{UB} - X_i \end{cases} \tag{7}$$

j. *Running back*: Move the current player back to its previous postion if it is fitter than the new position.

6. Return to step 3 and iterate the loop until a prescribed number of function evaluations; NFE_{max}, is completed.

Flowchart of the proposed algorithm is given in Fig. 1. Fixing the switching probability to 50%, STA works with the fewest control parameters; i.e. with N_p and NFE_{max}.

3. NUMERICAL SIMULATION

Performance of STA is evaluated here via comparison with some other literature works on a number of pin-jointed structures. The sizing probelm is formulated to find the least structural weight provided that stress and/or displacement constraints are satisfied. Applying an external penalty approach, the problem is formulated to maximize the fitness function as:

$$Max\ \ Fitness(X) = -Cost = -(1+\eta Q)\rho \sum_i l_i A_i \tag{8}$$

in which, l_i and A_i stand for the member length and cross-section area, respectively. The material density is denoted by ρ while η indicates the penalty factor; taken 10 in this study. Q takes into account the overall violation of constraints by:

$$Q = \max_k \{\max(0, g_k(X))\} \tag{9}$$

where any k^{th} constraint in the standard form is given by $g_k(X) \leq 0$. Dimension of the vector X is the same as the number of member groups; with a section index or area in each design variable x_j.

In order to perform fair comparison on the results in each problem, the following *Variation Index*; is determined and computed for each method:

$$VI = COV * NR * NFE / 1000 \tag{10}$$

Such a *VI* takes into account not only *Coefficient Of Variation* (*COV*; i.e. standard deviation divided by the mean) but also number of trial runs (*NR)* as well as number of function evaluations (*NFE*). Employing 40 total players in each example the number of iterations is given in its convergence curve; large enough to reach the corresponding NFE_{max}.

Table 1: Member groups and corresponding allowable stresses for 25-bar truss

Group Variable	Member Areas	Compressive Stress limit *ksi (MPa)*	Tensile Stress limit *ksi (MPa)*
X_1	A_1	35.092 (241.96)	40.0 (275.80)
X_2	A_2~A_5	11.590 (79.913)	40.0 (275.80)
X_3	A_6~A_9	17.305 (119.31)	40.0 (275.80)
X_4	A_{10}~A_{11}	35.092 (241.96)	40.0 (275.80)
X_5	A_{12}~A_{13}	35.092 (241.96)	40.0 (275.80)
X_6	A_{14}~A_{17}	6.759 (46.603)	40.0 (275.80)
X_7	A_{18}~A_{21}	6.959 (47.982)	40.0 (275.80)
X_8	A_{22}~A_{25}	11.082 (76.410)	40.0 (275.80)

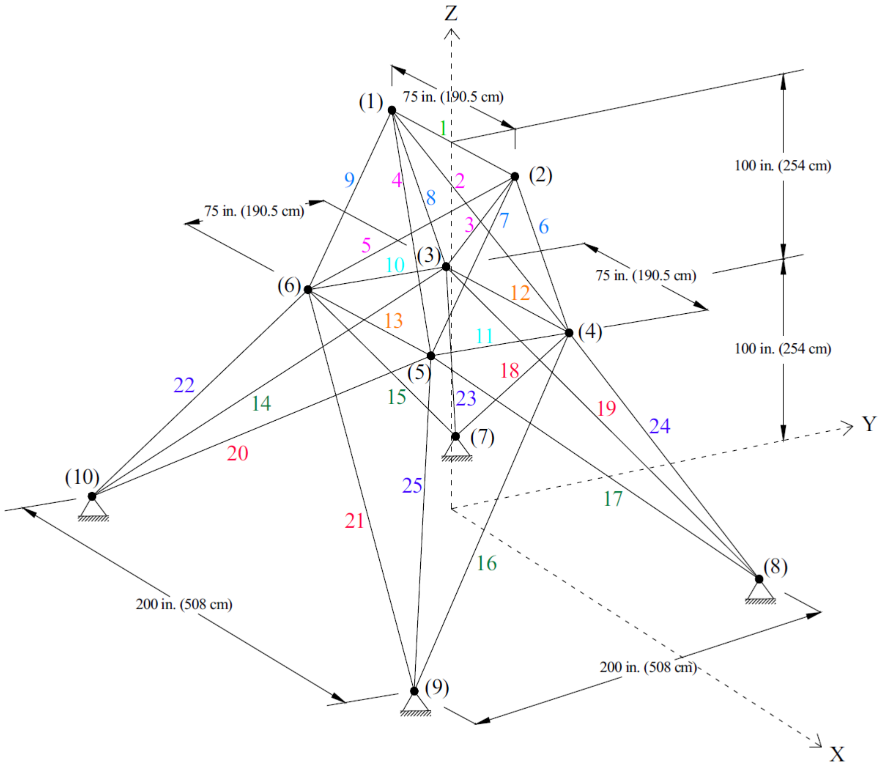

Figure 2. 25-bar space truss [22]

3.1 25-bar space truss

As a widely used benchmark to validate optimization algorithms, 25-bar power-transmission truss of Fig. 2 is treated [1]. The truss members are linked to 8 symmetric groups as given in Table 1. Material density is 0.1lb/in^3 (2767.99 kg/m^3) while it has elasticity modulus of 10000*ksi* (68.95*GPa*). Similar limit of 0.35*in* is imposed on nodal displacements in each orthogonal direction.

For the first experiment, section area of each member group is to be assigned within a continuous range from 0.01in^2 to 3.40in^2. Other behavior constraints include stress limits on tension members as 40.0*ksi* (275.80*MPa*) and those taking into account buckling effect on compression members are given in Table 1. In this experiment, the structure is supposed to distinctly resist two load cases of Table 2.

Table 2: Loading (*kips*) on 25-bar truss with continuous variables

	Case 1			*Case 2*		
Node	P_x	P_y	P_z	P_x	P_y	P_z
1	0.0	20.0	-5.0	1.0	10.0	-5.0
2	0.0	-20.0	-5.0	0.0	10.0	-5.0
3	0.0	0.0	0.0	0.5	0	0
6	0.0	0.0	0.0	0.5	0	0

*1kips=4.45kN

Table 3: Performance comparison in sizing of 25-bar spatial truss with continuous variables

Variable	**PSO**[31]	**MSPSO**[31]	**HPSSO**[32]	**IRO**[33]	**WEO**[22]	**ACO**[34]	**STA**
$\mathbf{X_1}$ (in^2)	0.0100	0.0100	0.0100	0.0112	0.0100	0.0100	0.0102
$\mathbf{X_2}$	1.9503	1.9848	1.9907	1.9766	1.9814	2.0000	1.9866
$\mathbf{X_3}$	3.0408	2.9956	2.9881	3.0099	3.0023	2.9660	2.9943
$\mathbf{X_4}$	0.0100	0.0100	0.0100	0.0100	0.0100	0.0100	0.0100
$\mathbf{X_5}$	0.0100	0.0100	0.0100	0.0100	0.0100	0.0120	0.0100
$\mathbf{X_6}$	0.6929	0.6852	0.6824	0.6842	0.6827	0.6890	0.6835
$\mathbf{X_7}$	1.6866	1.6778	1.6764	1.6783	1.6778	1.6790	1.6770
$\mathbf{X_8}$	2.6362	2.6599	2.6656	2.6571	2.6612	2.6680	2.6626
Best (*lb*)	545.22	545.16	545.16	545.19	545.16	545.53	545.16
Mean *(lb)*	549.96	546.03	545.56	545.35	545.23	546.34	552.43
NFE	25000	25000	18000	15000	20000	16500	12000
(NFE_best)	(18400)	(10800)	(13326)	(12200)	(19750)	(4700)	(11985)
NR	50	50	50	50	10	100	10
VI	22.52	1.83	0.71	N/A	0.03	2.84	3.10

VI: Variation Index, N/A: Not Available

According to Table 3, the proposed method has obtained the best result among the others regarding that no constraint violation has occurred. That is structural weight as small as 545.164*lb* within 11985 structural analyses. The required computational cost is also competitive with the others. However, applying 10 independent runs has led to greater mean result. The resulted VI of STA is very smaller than PSO but competitive to the others; where WEO has the first rank in this regard. Here, Fig. 3 reveals that STA has preserved a level of diversity so that during further iterations the mean result does not coincide with the best by a relatively stable margin.

According to Fig. 4, the displacement constraint is activated in both cases where stress ratio in case 1 has reached its limit. The matter declares success of the proposed algorithm in revealing constrained optimum.

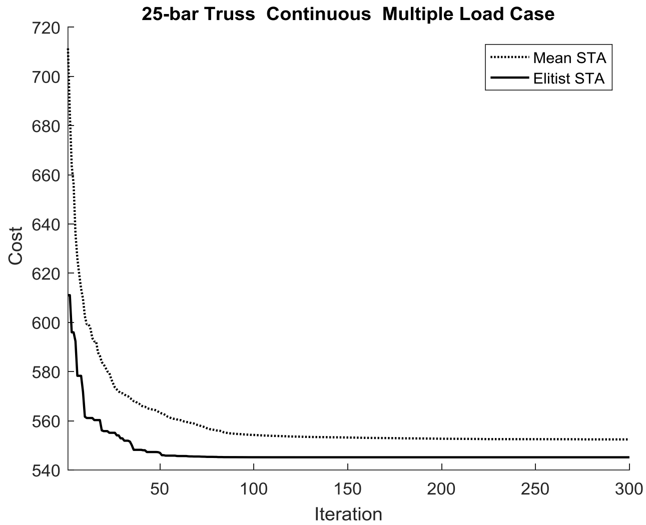

Figure 3. Convergence history of 25-bar truss design with continuous variables

For the second experiment, section areas are selected from a discrete list of 34 values from 0.1 to 3.40in^2 with interval of 0.1in^2. In this case, allowable compressive stress is similar to tensile stress; i.e. it is set to -40.0*ksi* and the structure undergoes single loading case given by Table 4.

Table 5 reports the results comparison of this example when dealing with discrete variables. In this case, STA has revealed the best feasible design with the weight of 484.328lb by less than 2000 structural analyses. It is better than the second rank belonging to ACO[34] that required 5200 analyses to achieve a truss weight of 484.85lb. In such a discrete problem, VI of STA has improved to 0.49 with respect to continuous design experiment. It is much better than VI of 7.46 by ACO. Convergence curves in this experiment on discrete sizing design of 25-bar truss are depicted in Fig. 5. A diversity margin is again oberved between the best and mean result of STA. It is evident from Fig. 6 that only displacement constraint is activated under such a single load case.

Table 4: Loading (*kips*) on 25-bar truss with discrete variables

	Case 1		
Node	P_x	P_y	P_z
1	0.0	-10.0	-10.0
2	1.0	-10.0	-10.0
3	0.6	0.0	0.0
6	0.5	0.0	0.0

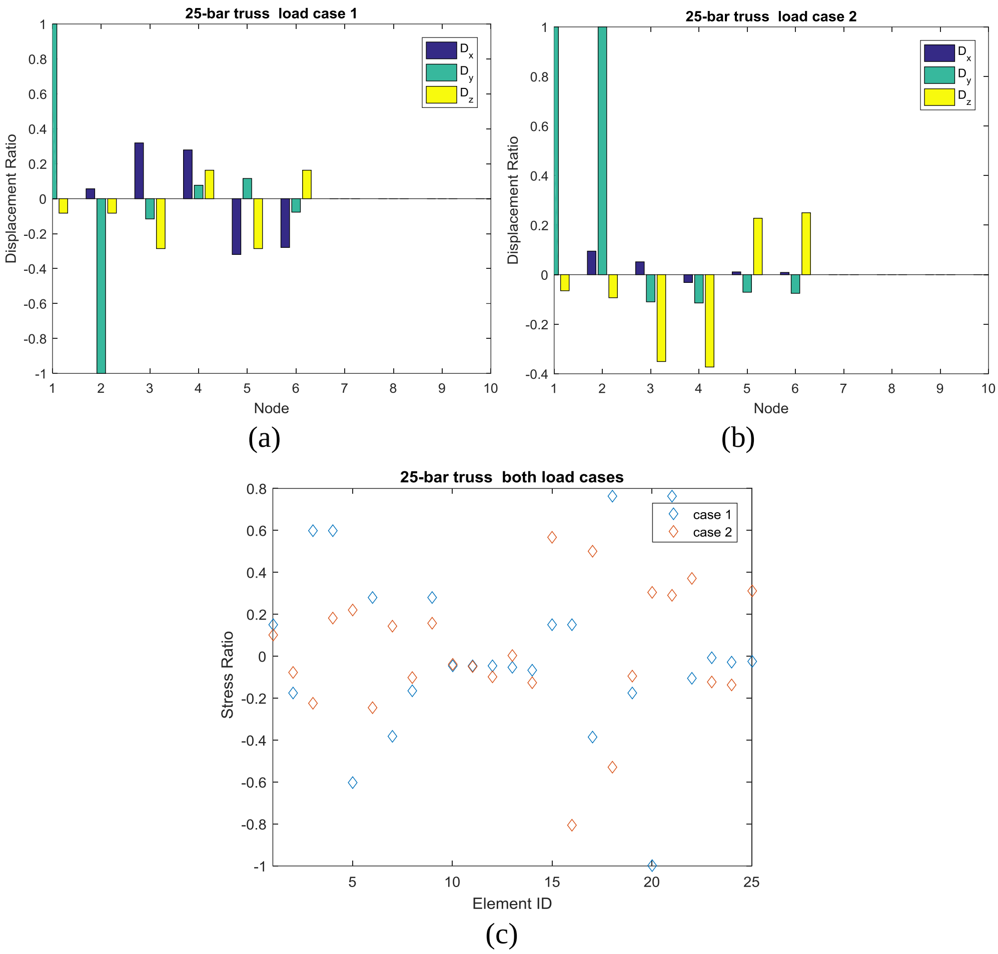

Figure 4. Structural responses of 25-bar truss: a) case 1, b)case2 , c)both load cases

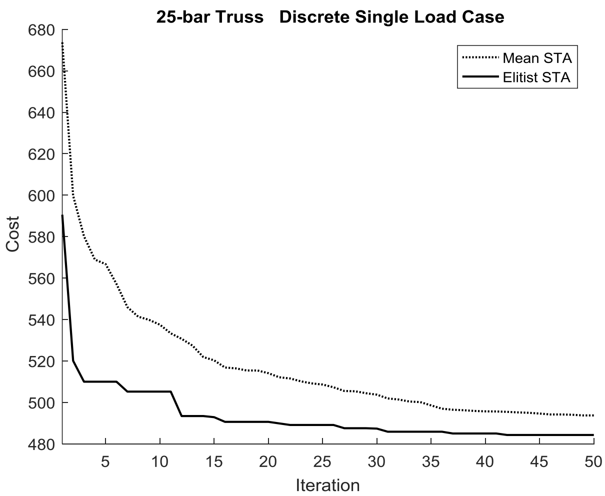

Figure 5. Convergence history of 25-bar truss design with discrete variables

Table 5: Performance comparison in sizing of 25-bar spatial truss with discrete variables

Variable	**GA** [1]	**GA** [35]	**IRO** [33]	**BB-BC** [36]	**ACO** [34]	**STA**
$\mathbf{X_1}$ (in^2)	0.1	0.1	0.1	0.1	0.1	0.1
$\mathbf{X_2}$	1.8	0.5	0.5	0.3	0.3	0.4
$\mathbf{X_3}$	2.3	3.4	3.4	3.4	3.4	3.4
$\mathbf{X_4}$	0.2	0.1	0.1	0.1	0.1	0.1
$\mathbf{X_5}$	0.1	1.9	1.9	2.1	2.1	2.2
$\mathbf{X_6}$	0.8	0.9	0.9	1.0	1.0	1.0
$\mathbf{X_7}$	1.8	0.5	0.5	0.5	0.5	0.4
$\mathbf{X_8}$	3.0	3.4	3.4	3.4	3.4	3.4
Best (*lb*)	546.01	485.05	485.05	484.85	484.85	484.328
Mean *(lb)*	N/A	N/A	484.90	485.10	486.46	493.656
NFE(best)	(800)	15000	(925)	(9000)	7700(5200)	2000(1677)
NR	N/A	N/A	50	N/A	100	10
VI	N/A	N/A	N/A	N/A	7.46	0.49

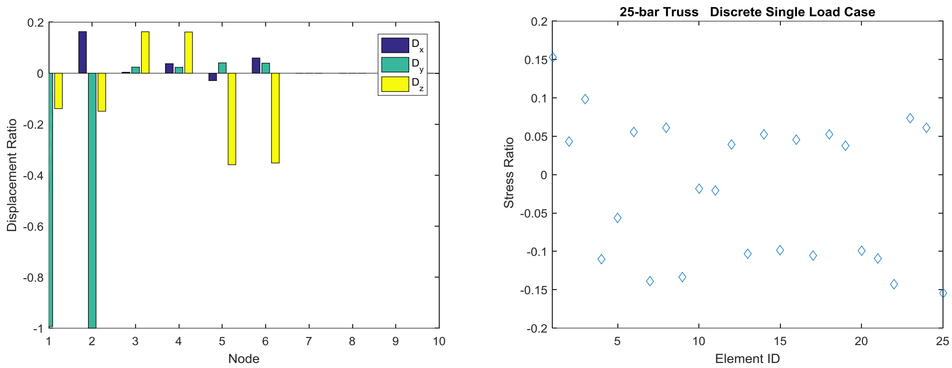

Figure 6. Structural responses of optimal 25-bar truss with discrete variables

3.2 47-bar power transmission

As a practical application, member areas of a power transmission truss (Fig. 7) is optimized by the proposed method. It was first considered for simultaneously size and geometry optimization by Flix and Vanderplaats [37], then addressed by others [38,39] under three distinct loading cases:

1. 6*kips* acting in positive *X*-direction and 14*kips* in negative *Y*-direction at nodes 17 and 22
2. The aforementioned loads exerted only on node 17
3. The aforementioned loads exerted only on node 22

The first case introduces, condition of two power lines attached to the tower at an angle. when each of these lines snaps the second and third loading cases occur. Lee et al. [39] also presented a solution of this problem for pure sizing under the third load case; which the same is concerned in the present study. Forty-seven members of the truss are linked to 27 sizing groups as given in Table 6. The section area of each group constitute a discrete design variable to be chosen from available list of Table 7.

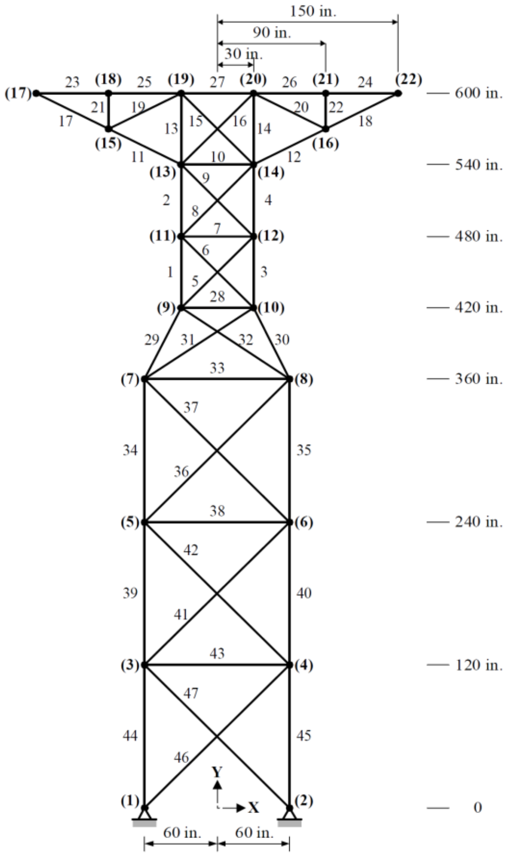

Figure 7. 47-bar power transmission tower [39]

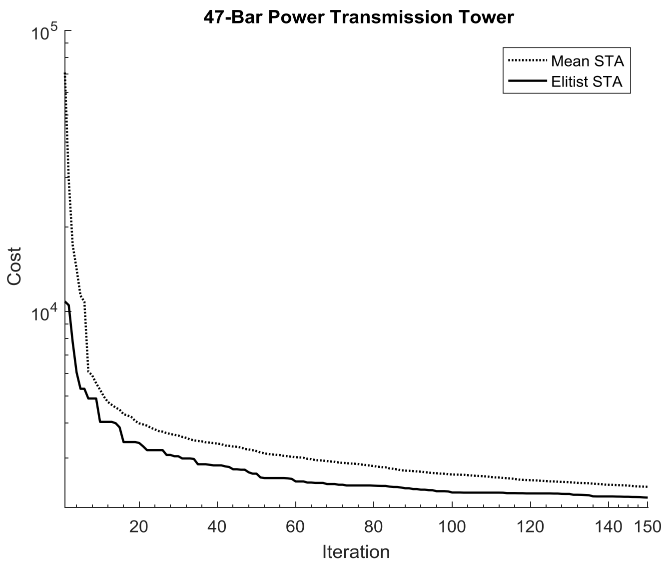

Figure 8. Convergence history of 47-bar truss design

Table 6: Member groups for sizing design of 47-bar tower

Group ID	Member Areas	Group ID	Member Areas	Group ID	Member Areas
1	A_1,A_3	**10**	A_{17},A_{18}	**19**	A_{33}
2	A_2,A_4	**11**	A_{19},A_{20}	**20**	A_{34},A_{35}
3	A_5,A_6	**12**	A_{21},A_{22}	**21**	A_{36},A_{37}
4	A_7	**13**	A_{23},A_{24}	**22**	A_{38}
5	A_8,A_9	**14**	A_{25},A_{26}	**23**	A_{39},A_{40}
6	A_{10}	**15**	A_{27}	**24**	A_{41},A_{42}
7	A_{11},A_{12}	**16**	A_{28}	**25**	A_{43}
8	A_{13},A_{14}	**17**	A_{29},A_{30}	**26**	A_{44},A_{45}
9	A_{15},A_{16}	**18**	A_{31},A_{32}	**27**	A_{46},A_{47}

Table 7: Discrete list of available section areas (in^2) for sizing design of 47-bar tower

ID	Area	ID	Area	ID	Area	ID	Area
1	0.111	**17**	1.563	**33**	3.840	**49**	11.500
2	0.141	**18**	1.620	**34**	3.870	**50**	13.500
3	0.196	**19**	1.800	**35**	3.880	**51**	13.900
4	0.250	**20**	1.990	**36**	4.180	**52**	14.200
5	0.307	**21**	2.130	**37**	4.220	**53**	15.500
6	0.391	**22**	2.380	**38**	4.490	**54**	16.000
7	0.442	**23**	2.620	**39**	4.590	**55**	16.900
8	0.563	**24**	2.630	**40**	4.800	**56**	18.800
9	0.602	**25**	2.880	**41**	4.970	**57**	19.900
10	0.766	**26**	2.930	**42**	5.120	**58**	22.000
11	0.785	**27**	3.090	**43**	5.740	**59**	22.900
12	0.994	**28**	3.130	**44**	7.220	**60**	24.500
13	1.000	**29**	3.380	**45**	7.970	**61**	26.500
14	1.228	**30**	3.470	**46**	8.530	**62**	28.000
15	1.266	**31**	3.550	**47**	9.300	**63**	30.000
16	1.457	**32**	3.630	**48**	10.850	**64**	33.500

The tower is made symmetric about Y-axis from steel with density of 0.3lb/in^3 and elasticity modulus of 30000*ksi*. Allowable stress is taken 20*ksi* for tensile members; however, its absolute is given by the following equation for compressive members taking into account the buckling stress:

$$\sigma_{compression}^{allowable} = \min \begin{cases} 15\,ksi \\ \dfrac{\kappa EA}{l^2}, \ \kappa = 3.96 \end{cases} \tag{11}$$

Table 8: Comparison of the results (section ID's) for 47-bar dome design

Var.	HS[39]	STA	Var.	HS[39]	STA	Var.	HS[39]	STA
X_1	33	25	X_{10}	21	18	X_{19}	6	24
X_2	29	23	X_{11}	1	1	X_{20}	27	28
X_3	10	18	X_{12}	1	21	X_{21}	16	14
X_4	2	10	X_{13}	19	19	X_{22}	3	1
X_5	11	9	X_{14}	19	19	X_{23}	33	27
X_6	20	17	X_{15}	16	15	X_{24}	17	14
X_7	21	21	X_{16}	7	1	X_{25}	3	1
X_8	14	12	X_{17}	32	25	X_{26}	39	30
X_9	17	15	X_{18}	16	14	X_{27}	16	14
Best (*lb*)							2396.8	2172.49
Mean *(lb)*							N/A	2372.75
NFE(best)							(45557)	6000(5991)
NR							N/A	10
VI							N/A	3.98

Convergence curve of Fig. 8 reveals great drop of the cost function (structural weight) and its continued refinement in iterations of the search by STA. The curve is demonstrated in logarithmic scale to better declare such an improvement and also the difference between the best and mean results during optimization.

Table 8 reports superior performance of STA over HS in such a pure sizing discrete design. In this example, STA has captured best weight of 2172.49*lb* by just 6000 structural analyses. It is 10% lighter than the result of the other literature work that has achieved 2396.8*lb* within 7.6 times more computational effort than STA. Fig. 9 declares how the behavior constraint in the optimal design of 47-bar tower, is activated by STA.

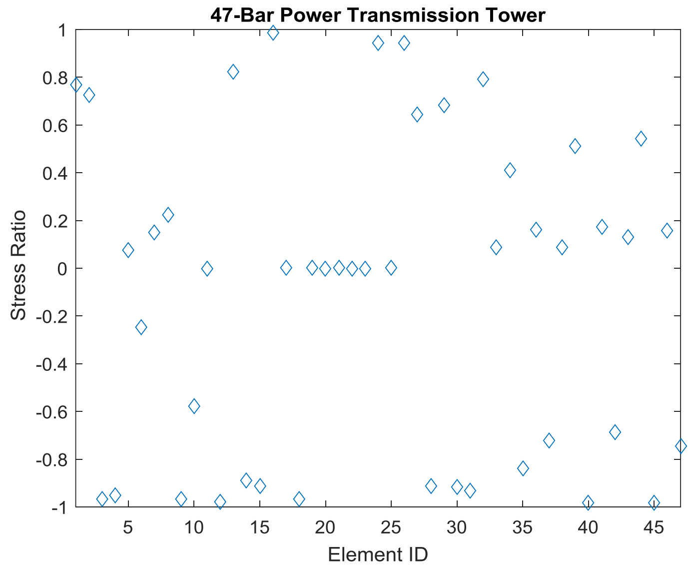

Figure 9. Structural responses of optimal 47-bar truss design

3.3 120-bar dome

As a widely used continuous structural problem, weight minimization of the spatial dome (Fig. 10) is concerned [9,40]. Continuous design variables include section areas for seven element groups within the range 0.775 to 20.000 in^2. The employed material has density of 0.288*lb/in*^{3}, elasticity modulus of 30450*ksi* and yield stress of 58*ksi*.

Structural loading consists of 13.489*kips* at node 1, 6.744 *kips* at nodes 2 to 13 and 2.248*kips* at the other free nodes. Pipe sections are utilized so that gyration radii can be extracted from area by $r = 0.4993A^{0.6777}$. Allowable stress design provisions of the practice code[41,42] is applied as:

$$\sigma_{tension}^{allowable} = 0.6F_y \tag{12}$$

$$\sigma_{compression}^{allowable} = \begin{cases} \dfrac{12\pi^2 E}{23\lambda^2} & \text{for } \dfrac{\lambda}{C_c} \geq 1 \\ (1 - \dfrac{\lambda^2}{2{C_c}^2})F_y \Big/ (\dfrac{5}{3} + \dfrac{3}{8}\dfrac{\lambda}{C_c} - \dfrac{\lambda^3}{8{C_c}^3}) & \text{for } \dfrac{\lambda}{C_c} < 1 \end{cases} \tag{13}$$

$$C_c = \sqrt{2\pi^2 E \big/ F_y}$$

where λ denotes slenderness ratio of the corresponding member. It is calculated using effective length divided by section gyration radius. As the structure include truss members, their buckling length factor is unity.

This example has already been addressed by several investigators when its original case is treated here. Some of their related works are reported in Table 9. STA has captured a feasible design weighing 19473.27*lb*; that is 0.1% heavier than the best result by CBO among the others. However, such a result of STA has been obtained via 7643 analyses much lower than 14960 structural analyses by CBO. As can be realized in Fig. 11, search improvement of STA occurs after early cost-drop in initial iterations. According to Fig. 12, STA has also been successful in activating the stress constraint in optimal design.

Table 9: Comparison of the results for 120-bar dome design

	HS[9]	**HPSACO**[11]	**RO**[43]	**CBO**[40]	**ICLBO**[18]	**STA**
X_1 (*in*^{2})	3.295	3.311	3.128	3.123	3.124	3.1220
X_2	2.396	3.438	3.357	3.354	3.454	3.3710
X_3	3.874	4.147	3.874	4.112	4.113	4.1143
X_4	2.571	2.831	4.114	2.782	2.786	2.7819
X_5	1.150	0.775	0.775	0.775	0.775	0.7865
X_6	3.331	3.474	3.302	3.300	3.573	3.3004
X_7	2.784	2.551	2.453	2.446	2.446	2.4456
Best (*lb*)	19707.8	19491.3	19476.2	19454.7	19680.6	19473.27
Mean *(lb)*	N/A	N/A	N/A	19466.0	23661.0	20064.89
NFE(best)	50000	10000	(19950)	(14960)	30000	8000
NR	N/A	50	30	20	10	10
VI	N/A	N/A	N/A	N/A	38.0	3.3

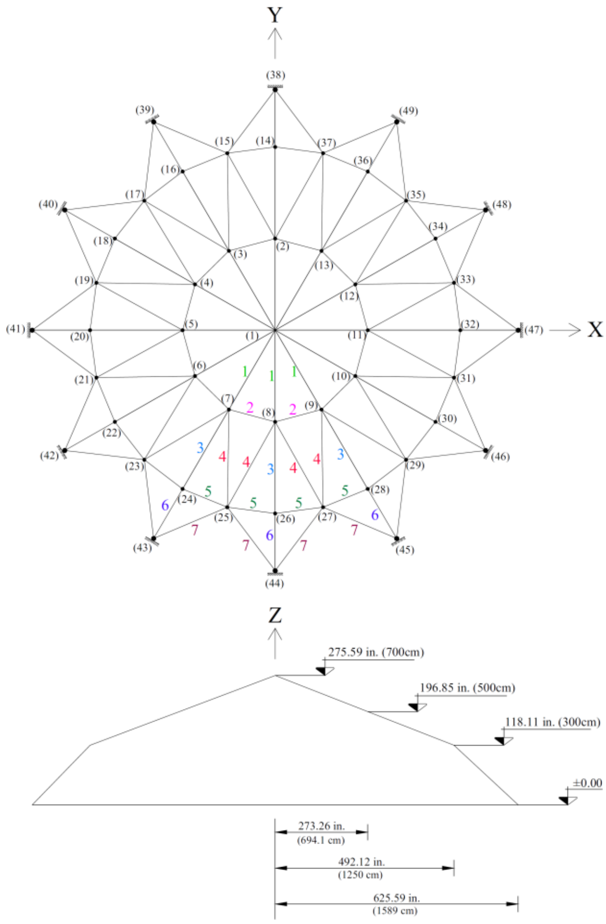

Figure 10. 120-bar dome truss [22]

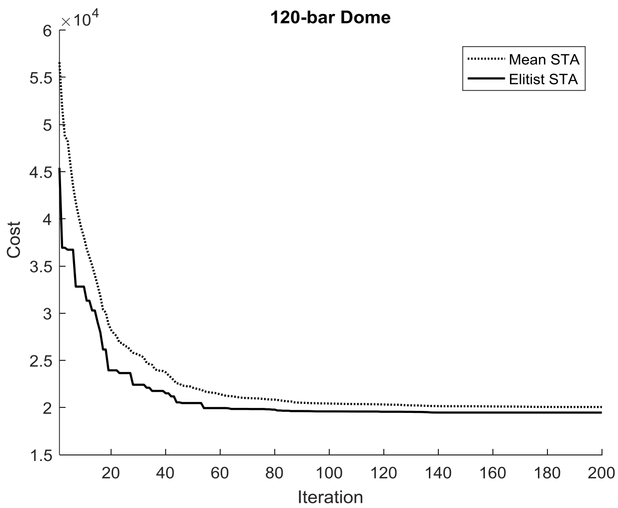

Figure 11. Convergence history of 120-bar dome

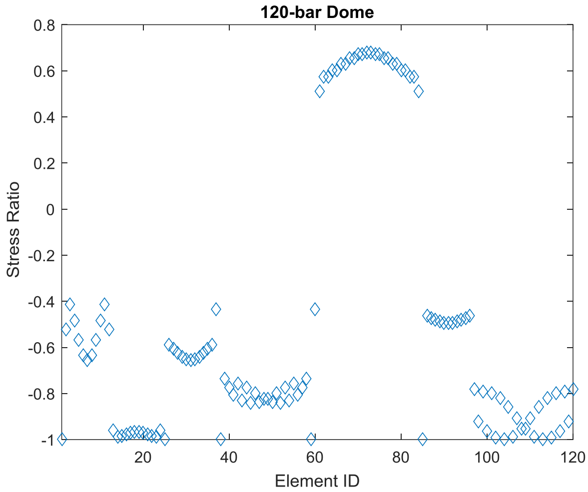

Figure 12. Structural responses of optimal 120-bar dome design

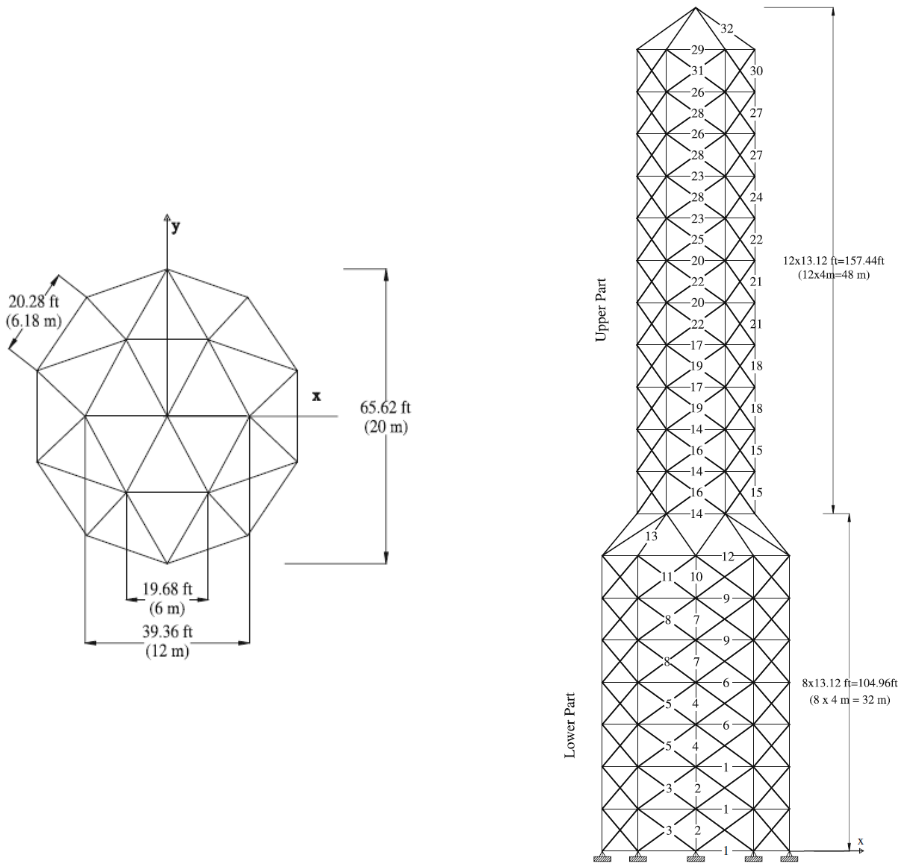

(a) (b)

Figure 13. 582-bar tower: (a) Top view, (b)Side view [44]

3.4 582-bar tower

Performance of the proposed method in optimal design of a large scale benchmark is evaluated in this example. The 80*m* tower has 582 pin-jointed elements linked to 32 symmetric groups as given in literature. Geometry and topology of the 582-bar tower truss is demonstrated in Fig. 13. Elasticity modulus is 204*MPa* while the yield stress is taken 253.1*MPa*. The tower resists a single load case including lateral loads of 5*kN* in X and Y directions while each node undergoes a downward load of 30*kN*.

Nodal displacements are confined to 0.08*m* in each direction. Members are subjected to allowable stress design regulations of the practice code with Equations (12) and (13). Additional limits of 200 and 300 are exerted on the slenderness ratio in compressive and tensile elements, respectively.

The problem is treated with integer section indices as discrete design variables. Some investigators applied a set of 137 economical standard steel W-shape profiles with section areas between $6.16in^2$ ($39.74cm^2$) and $215.0in^2$ ($1387.09cm^2$) [45]. However, in the present work a list of 140 W-Sections are utilized as given by Sonmez [44]. Consequently, the search space will be of the order 10^{68} that is considerably large. The objective (cost) function is taken total volume over the structural members.

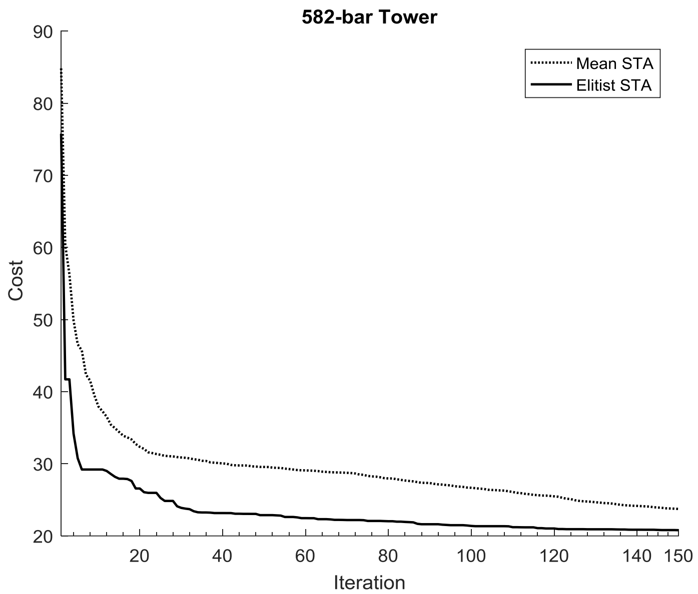

Figure 14. Convergence history of 582-bar tower

The proposed STA has captured the best design with a volume of $21.13m^3$; superior to other literature works in Table 10. Such a result has been achieved via just 5985 function evaluations by STA, while the best result among the others; i.e. CBO required 6400 structural analyses to obtain a greater volume of $21.838m^3$.

Table 10: Comparison of the results for 582-bar tower design

Group	**PSO**[45]	**BB-BC**[46]	**DHPSACO**[8]	**CBO**[47]	**STA**
1	W8x21	W8x24	W8x24	W8x21	W8x21
2	W12x79	W24x68	W12x72	W12x79	W10x68
3	W8x24	W8x28	W8x28	W8x28	W8x21
4	W10x60	W18x60	W12x58	W10x60	W10x77
5	W8x24	W8x24	W8x24	W8x24	W8x21
6	W8x21	W8x24	W8x24	W8x21	W8x21
7	W8x48	W21x48	W10x49	W10x68	W10x60
8	W8x24	W8x24	W8x24	W8x24	W8x21
9	W8x21	W10x26	W8x24	W8x21	W8x21
10	W10x45	W14x38	W12x40	W14x48	W14x48
11	W8x24	W12x30	W12x30	W12x26	W8x21
12	W10x68	W12x72	W12x72	W21x62	W14x74
13	W14x74	W21x73	W18x76	W18x76	W16x67
14	W8x48	W14x53	W10x49	W12x53	W12x65
15	W18x76	W18x86	W14x82	W14x61	W12x65
16	W8x31	W8x31	W8x31	W8x40	W8x21
17	W8x21	W18x60	W14x61	W10x54	W12x65
18	W16x67	W8x24	W8x24	W12x26	W8x21
19	W8x24	W16x36	W8x21	W8x21	W8x21
20	W8x21	W10x39	W12x40	W14x43	W10x68
21	W8x40	W8x24	W8x24	W8x24	W8x21
22	W8x24	W8x24	W14x22	W8x21	W8x21
23	W8x21	W8x31	W8x31	W10x22	W10x22
24	W10x22	W8x28	W8x28	W8x24	W8x21
25	W8x24	W8x21	W8x21	W8x21	W12x40
26	W8x21	W8x24	W8x21	W8x21	W6x25
27	W8x21	W8x28	W8x24	W8x24	W10x22
28	W8x24	W14x22	W8x28	W8x21	W8x21
29	W8x21	W8x24	W16x36	W8x21	W8x28
30	W8x21	W8x24	W8x24	W6x25	W10x22
31	W8x24	W14x22	W8x21	W10x33	W16x36
32	W8x24	W8x24	W8x24	W8x28	W12x53
Best (m^3)	22.396	22.371	22.061	21.838	21.130
Mean (m^3)	N/A	N/A	23.410	N/A	23.738
NFE(best)	50000	12500	(8500)	(6400)	6000(5985)
NR	N/A	N/A	20	N/A	10
VI	N/A	N/A	12.1	N/A	6.9

The study also reveals comparable VI of STA with the others, in this example. For such a problem with high cardinality of search space, convergence history of STA are given in Fig. 14; where a decreasing trend of mean volume (cost function) is observed with a difference from the best result. At the optimal design by STA, the maximum stress ratio is lower than 80%. Meanwhile activation of the displacement can be observed in Fig. 15.

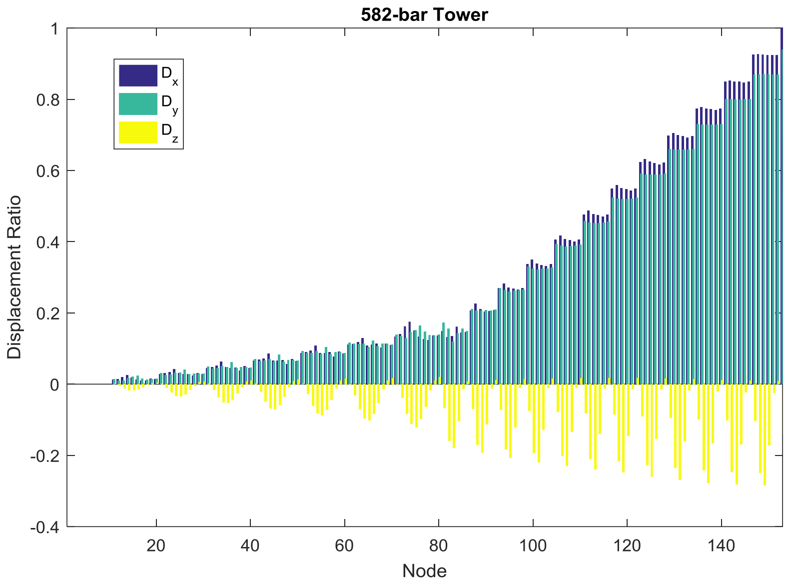

Figure 15. Structural responses of optimal 582-bar tower design

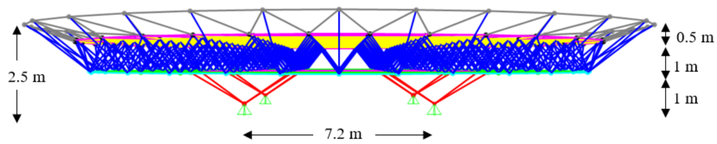

Figure 16. 1104-bar helipad structure [18]

3.5 1104-bar helipad

The helipad truss of Fig. 16 with diameter of 21*m* in the outer top ring and 18*m* in the inner ring is considered for sizing design. The structure is made of steel with density of 7850*kg/m*^{3}, elasticity modulus of 203.9*GPa* where the yield stress is 235.1*MPa*. Geometry and member grouping of this practical example have been given in literature [18].

Each of the four central nodes, undergoes a point load of 350*kgf* in negative vertical direction while a uniform load of 300*kgf/m*^{2} is applied on the top level. Nodal displacements are confined within 0.005*m*. Meanwhile, stress constraints are given by with Equations (12) and (13). Section areas for 9 symmetric member group can continuously be chosen between 10*cm*^{2} and 100*cm*^{2}.

Fig. 17 shows STA convergence to a solution of this example in 100 iterations. In another word, within 3997 structural analyses STA has captured the structural weight of 25723.73*kg*. It is superior to the results of *Teaching Learning-Based Optimization* [48], *Ant Lion Optimizer* [49], *Thermal Exchange Optimization* [23] and Whale Optimization Algorithm[50], as reported in Table 11. Such superiority is observed not only in the best but also in the mean result of STA; while its VI stands in the middle rank. It is also evident from Fig. 18 that displacement constraint is successfully activated by STA.

Table 11: Comparison of the results for 1104-bar helipad design

	TLBO	ALO	TEO	WOA	STA
A1(cm^2)	16.78	36.19	18.49	28.57	16.17
A2	31.24	26.55	29.63	25.62	31.80
A3	53.61	41.55	67.88	48.86	49.37
A4	10.63	11.01	10.00	10.00	10.96
A5	26.85	27.64	25.54	47.81	26.22
A6	10.29	11.18	10.00	10.23	10.04
A7	22.46	29.51	30.85	11.69	20.89
A8	10.11	11.05	10.34	10.00	10.03
A9	81.09	71.95	72.05	84.15	87.20
Best (*kg*)	25761.48	26632.82	26017.72	27714.31	25723.73
Mean(*kg*)	26678.20	27466.38	26539.29	33594.71	26348.68
NFE	4000	4000	4000	4000	4000
NR	10	10	10	10	10
VI	1.20	1.08	0.43	4.11	1.12

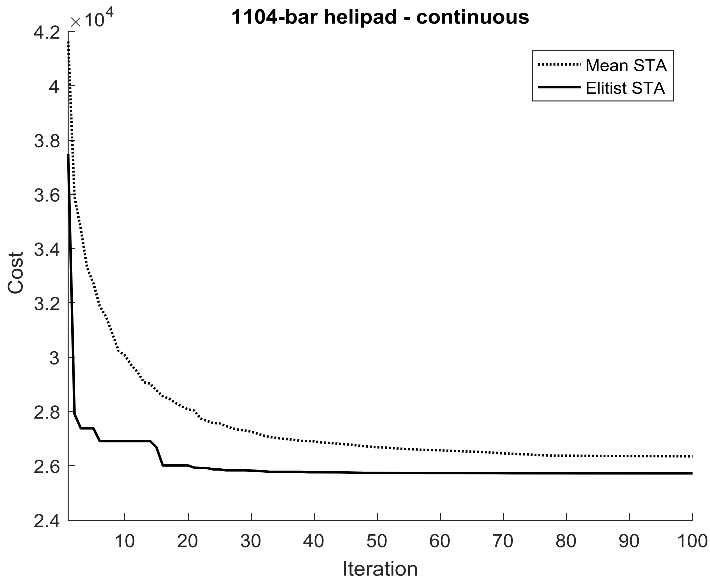

Figure 17. Convergence curves of 1104-bar helipad design

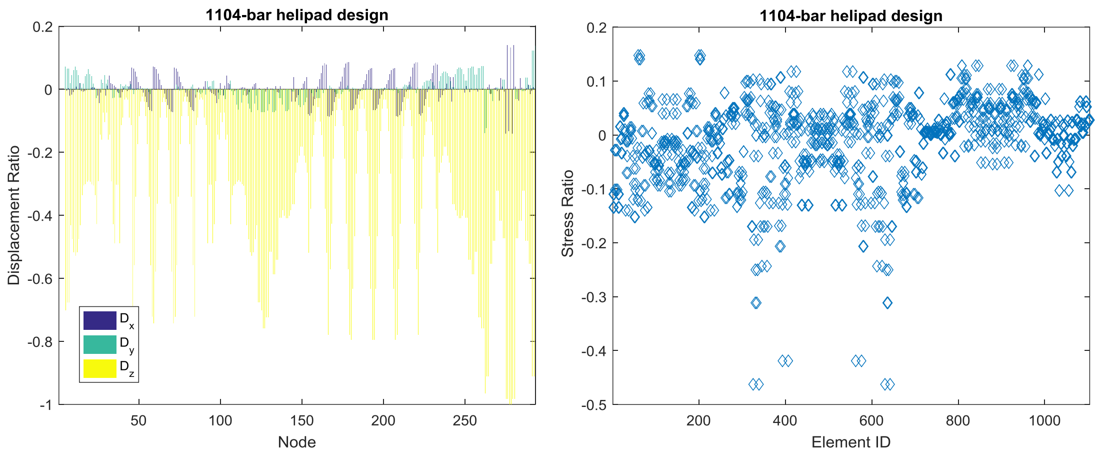

Figure 18. Structural responses of optimal 1104-bar tower design

4. DIVERSITY STUDY AND DISCUSSION

In order to better study behavior of STA, variantion of player position is averaged over the entire population by the following measure:

$$MVN = \frac{1}{N_p}\sum_{i=1}^{N_p}\left\| X_i^{New} - X_i^{Old} \right\| \quad (14)$$

Tracing such an index among iterations of the algorithm, will give further insight on its behavior. The index will approach zero when all the players tend to stop at their final positions; i.e. the algorithm converges to the solution state. However, it is not the case at early iterations of the methd when it is discovering differnt regions of the search space. In another word, tracing MVN declares how a meta-heuristic algorithm changes from more exploration to more exploitation (convergence) during iterations of the search.

Such a study is perfomed for the treated examples and the results are demonstrated in Fig. 19. Differences are observed in MVN curves when the problem is changed; that means STA can robustly change its trend of diversity variation case by case. As an interesing example, consider two verisons of 25-bar truss optimization problem; i.e. the discrete and the continuous version. According to Fig. 19, MVN curves differ between the aforemnetioned cases: at final iterations of continuous problem MVN is approaching zero but it continues to show considerable fluctuations in the discrete 25-bar design problem. Similar phenomenon is declared (more or less) between other treated discrete and continuous examples in Fig. 19. A common trend is observed among these problems; STA starts with a high diversity, experiences considerable drop at some early iterations and continues with lower overall diversity up to the convergence.

In most cases, STA shows some fluctuations during decreasing MVN; however, problem complexity or its discrete/coninuous type can alter the bandwidth of such fluctuations and their frequency of occurence. Capturing high quality optima in these examples confirms effectiveness of such diversity preservation in escaping from local optima traps.

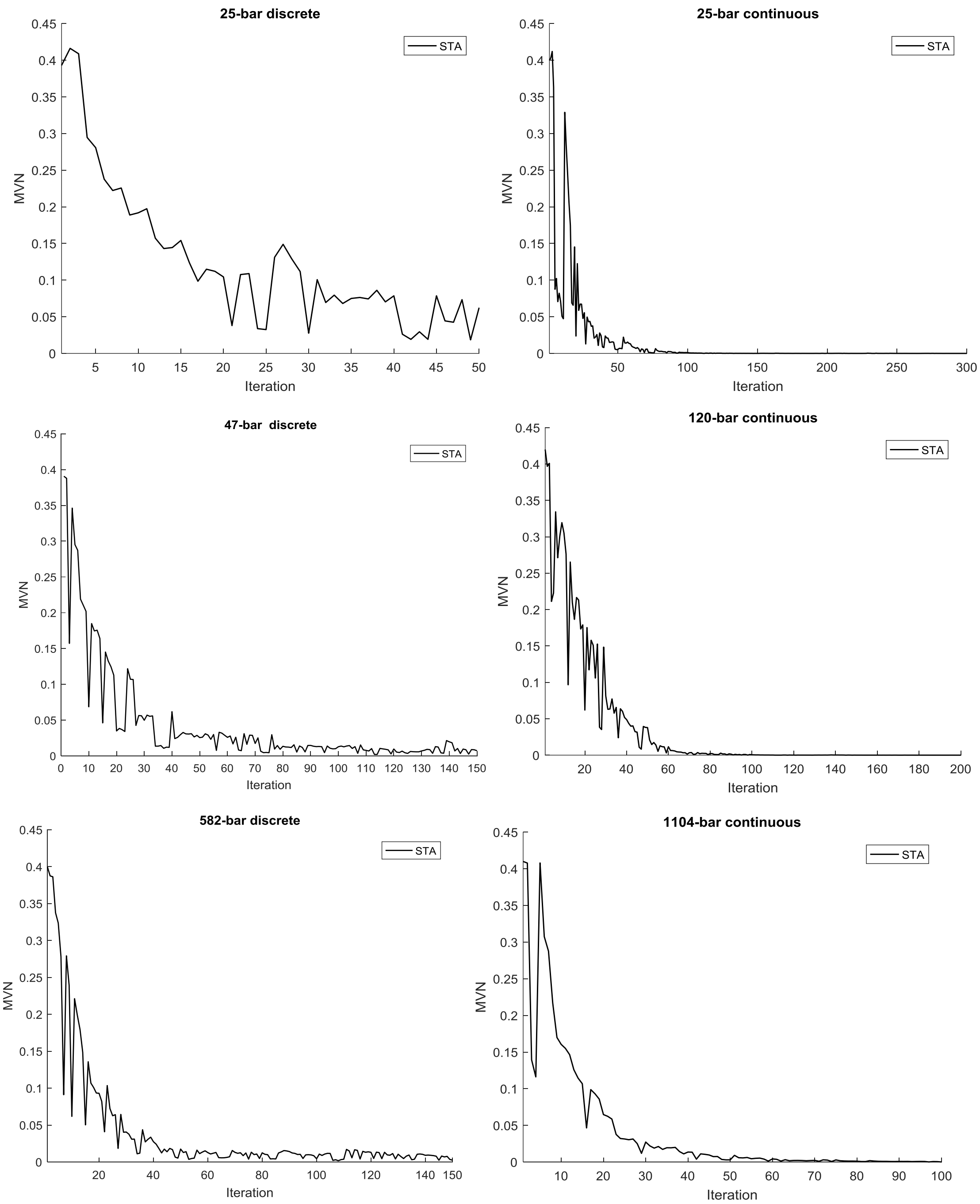

Figure 19. MVN variation trends in the treated examples

5. CONCLUSION

A novel meta-heuristic method is developed based on some player actions in two competting teams on the opposite sides. It was applied to a number of literature benchmarks in rewarding field of structural sizing design, in a variaty of small to large-scale and discrete/continuous constrained problems.

The proposed meta-heuristic algorithm exhibited competitive performance with the other treated literature works in capturing optimal sizing designs. Higher quality designs of STA were observed particularly in discrete and larger-scale structural examples. STA obtained such results with lower computational effort than the others. Activating stress or displacemet constraints in each problem confirms optimality of the solution revealed by STA.

Since literature works were run with differnet number of runs or structural analyses, a variation index is utilized for better comparison of their robustness. According to the results STA is distinguished with moderate VI and even first rank in some cases. Note that the proposed method utilizes just two common control parameters. Reducing the parameter tuning effort can in charge affect the problem-specific search refinement. Nevertheless, STA has escaped from local optima in the studied examples revealing high quality solutions with respect to the others. The empoyed switching opertaors in the algorithm view have led to fluctuating behavior in the diversity view; that provides theoretical support for such numerical observations.

In the light of the present study, an interesting method has been offerred for optimization of constrained problems; specially when diversity maintenance is desired to overpass local optima.

REFERENCES

1. Rajeev S, Krishnamoorthy CS. Discrete optimization of structures using genetic algorithms, *J Struct Eng* 1992; **118**: 1233-50. doi:10.1061/(ASCE)0733-9445(1992)118.
2. Kaveh A, Shahrouzi M. An efficient stochastic search with minimal intial population for structural optimization, *Asian J Civ Eng* 2010; **11**: 741–62.
3. Shahrouzi M, Sardarinasab S. A new memtic swarm optimization for spectral layout design of braced frames, *Int J Optim Civ Eng* 2015; **5**: 53-65.
4. Papadrakakis M, Lagaros ND. Advanced solution methods in structural optimization based on evolution strategies, *Eng Comput* 1998; **15**: 12–34.
5. Lamberti L. An efficient simulated annealing algorithm for design optimization of truss structures, *Comput Struct* 2008; **86**: 1936–53.
6. Kaveh A, Azar BF, Hadidi A, Sorochi FR, Talatahari S. Performance-based seismic design of steel frames using ant colony optimization, *J Constr Steel Res* 2010; **66**: 566-74.
7. Pholdee N, Bureerat S. Comparative performance of meta-heuristic algorithms for mass minimisation of trusses with dynamic constraints, *Adv Eng Softw* 2014; **75**: 1-13.
8. Kaveh A, Talatahari S. A particle swarm ant colony optimization for truss structures with discrete variables, *J Constr Steel Res* 2009; **65**: 1558-68.

9. Lee KS, Geem ZW. A new structural optimization method based on the harmony search algorithm, Comput Struct 2004; **82**: 781–98.
10. Geem ZW, Lee KS. Harmony Search for Structural Design, *Gecco* 2005: 651–2.
11. Kaveh A, Talatahari S. Particle swarm optimizer, ant colony strategy and harmony search scheme hybridized for optimization of truss structures, *Comput Struct* 2009; **87**: 267–83.
12. Zhang T. *Overview of Applications and Developments in the Harmony Search Algorithm*, 2015.
13. Kaveh A, Talatahari S. Optimization of large-scale truss structures using charged system search, *Int J Optim Civ Eng* 2011; **1**: 15-28.
14. Kaveh A, Motie Share MA, Moslehi M. Magnetic charged system search: A new meta-heuristic algorithm for optimization, *Acta Mech* 2013; **224**: 85-107.
15. Kaveh A. *Advances in Metaheuristic Algorithms for Optimal Design of Structures*, Second edition, 2016.
16. Kaveh A, Mahdavi VR. *Colliding Bodies Optimization: Extensions and Applications*, 2015.
17. Bahrami H, Abdechiri M, Meybodi MR. Imperialist competitive algorithm with adaptive colonies movement, *Int J Intell Syst Appl* 2012; **4**: 49-57.
18. Shahrouzi M, Salehi A. Imperialist competitve learner-based optimization: a hybrid method to solve engineering problems, *Int J Optim Civ Eng* 2020; **10**: 155-80.
19. Talatahari S, Kaveh A, Sheikholeslami R. Chaotic imperialist competitive algorithm for optimum design of truss structures, *Struct Multidiscip Optim* 2012; **46**: 355-67.
20. Shahrouzi M, Meshkat-dini A, Azizi A. Simultaneous geometry and size optimization of diagrids against equivalent wind loading, *Adv Environ Mater Res*, ACEM16, JEJU, South Korea, 31Aug-1Sep: Techno-Press, 2016.
21. Degertekin SO, Hayalioglu MS. Sizing truss structures using teaching-learning-based optimization, *Comput Struct* 2013; **119**: 177–88.
22. Kaveh A, Bakhshpoori T. A new metaheuristic for continuous structural optimization: water evaporation optimization, *Struct Multidiscip Optim* 2016; **54**: 23-43.
23. Kaveh A, Dadras A. A novel meta-heuristic optimization algorithm: Thermal exchange optimization, *Adv Eng Softw* 2017; **110**: 69-84.
24. Mirjalili S, Mirjalili SM, Lewis A. Grey wolf optimizer, *Adv Eng Softw* 2014; **69**: 46-61.
25. Gandomi AH. Interior search algorithm (ISA): A novel approach for global optimization, *ISA Trans* 2014; **53**: 1168-83.
26. Gandomi AH, Yang XS, Alavi AH. Cuckoo search algorithm: A metaheuristic approach to solve structural optimization problems, *Eng Comput* 2013; **29**: 17–35.
27. Mirjalili S. SCA: A Sine Cosine Algorithm for solving optimization problems, *Knowledge Based Syst* 2016; **96**: 120–33.
28. Gholizadeh S, Sojoudizadeh R. Modified sine-cosine algorithm for sizing optimization of truss structures with discrete design variables, *Int J Optim Civil Eng* 2019; **9**: 195-212.
29. Kaveh A, Ghazaan MI. A new meta-heuristic algorithm : vibrating particles system, *Sci Iran* 2017; **24**: 1–32.
30. Črepinšek M, Liu S-H, Mernik M. Exploration and exploitation in evolutionary algorithms, *ACM Comput Surv* 2013; **45**: 1-33.
31. Talatahari S, Kheirollahi M, Farahmandpour C, Gandomi AH. A multi-stage particle swarm for optimum design of truss structures, Neural Comput Appl 2013; **23**: 1297-309.

32. Kaveh A, Bakhshpoori T, Afshari E. An efficient hybrid particle swarm and swallow swarm optimization algorithm, *Comput Struct* 2014; **143**: 40-59.
33. Kaveh A, Ilchi Ghazaan M, Bakhshpoori T. An improved ray optimization algorithm for design of truss structures, *Period Polytech Civil Eng* 2013; **57**: 97–112.
34. Camp C, Bichon B. Design of space trusses using ant colony optimization, *Struct Eng* 2004; **130**: 741-51.
35. Camp C, Pezeshk S, Cao G. Optimized design of two-dimensional structures using a genetic algorithm, *J Struct Eng* 1998; **124**: 551-9.
36. Kaveh A, Talatahari S. Size optimization of space trusses using Big Bang-Big Crunch algorithm, *Comput Struct* 2009; **87**: 1129-40.
37. Felix J, Vanderplaats GN. Configuration optimization of trusses subject to strength, displacement and frequency constraints, *J Mech Des Trans ASME* 1987; **109**: 233-41.
38. Hansen SR, Vanderplaats GN. Approximation method for configuration optimization of trusses, *AIAA J* 1990; **28**: 161–8.
39. Lee K, Han S, Geem Z. Discrete size and discrete-continuous configuration optimization methods for truss structures using the harmony search method, *Int J Optim Civil Eng* 2011; **1**: 107–26.
40. Kaveh A, Mahdavi VR. Colliding bodies optimization : A novel meta-heuristic method, *Comput Struct* 2014; **139**: 18–27.
41. AISC. *American Construction Institutes of Steel*, Manual of steel construction, Allowable Stress Design, 9th ed, Chicago, Illinois, 1989.
42. INBC: Part-10. Iranian National Building Code, Part-10: Design of Steel Structures, 4th ed. Tehran: Roads, Housing and Urban Development of Iran, 2013.
43. Kaveh A, Khayatazad M. A new meta-heuristic method: Ray Optimization, *Comput Struct* 2012; **112-113**: 283–94.
44. Sonmez M. Discrete optimum design of truss structures using artificial bee colony algorithm, *Struct Multidiscip Optim* 2011; **43**: 85–97.
45. Hasançebi O, Çarbaş S, Doğan E, Erdal F, Saka MP. Performance evaluation of metaheuristic search techniques in the optimum design of real size pin jointed structures, *Comput Struct* 2009; **87**: 284-302.
46. Kaveh A, Talatahari S. A discrete Big Bang - Big Crunch algorithm for optimal design of skeletal structures, *Asian J Civil Eng* 2010; **11**: 103–22.
47. Kaveh A, Mahdavi VR. *Colliding Bodies Optimization: Extensions and Applications*, Springer International Publishing, 2015.
48. Rao RV, Savsani VJ, Vakharia DP. Teaching-Learning-Based Optimization: An optimization method for continuous non-linear large scale problems, *Inform Sci (Ny)* 2012; **183**: 1-15.
49. Mirjalili S. The ant lion optimizer, *Adv Eng Softw* 2015; **83**: 80–98.
50. Mirjalili S, Lewis A. The whale optimization algorithm, *Adv Eng Softw* 2016; **95**: 51-67.